

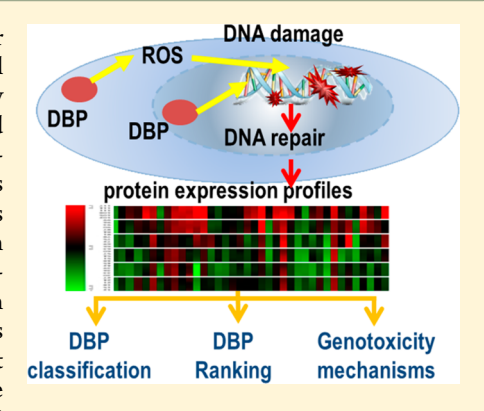
pubs.acs.org/est

# Genotoxicity Assessment of Drinking Water Disinfection Byproducts by DNA Damage and Repair Pathway Profiling Analysis

Jiaqi Lan, † Sheikh Mokhlesur Rahman, † Na Gou, † Tao Jiang, † Micheal J. Plewa, \* Akram Alshawabkeh,† and April Z. Gu\*,†,||®

# Supporting Information

ABSTRACT: Genotoxicity is considered a major concern for drinking water disinfection byproducts (DBPs). Of over 700 DBPs identified to date, only a small number has been assessed with limited information for DBP genotoxicity mechanism(s). In this study, we evaluated genotoxicity of 20 regulated and unregulated DBPs applying a quantitative toxicogenomics approach. We used GFPfused yeast strains that examine protein expression profiling of 38 proteins indicative of all known DNA damage and repair pathways. The toxicogenomics assay detected genotoxicity potential of these DBPs that is consistent with conventional genotoxicity assays end points. Furthermore, the high-resolution, realtime pathway activation and protein expression profiling, in combination with clustering analysis, revealed molecular level details in the genotoxicity mechanisms among different DBPs and enabled classification of DBPs based on their distinct DNA damage effects and repair mechanisms. Oxidative DNA damage and base alkylation were confirmed to be the main molecular mechanisms of DBP



genotoxicity. Initial exploration of QSAR modeling using moleular genotoxicity end points (PELI) suggested that genotoxicity of DBPs in this study was correlated with topological and quantum chemical descriptors. This study presents a toxicogenomicsbased assay for fast and efficient mechanistic genotoxicity screening and assessment of a large number of DBPs. The results help to fill in the knowledge gap in the understanding of the molecular mechanisms of DBP genotoxicity.

# ■ INTRODUCTION

Drinking water disinfection byproducts (DBPs) are formed during the reaction of disinfectants (such as chlorine, chlorine dioxide, chloramine, UV, and ozone) with naturally occurring organic matter (NOM) and other contaminants present in water. DBPs therefore widely exist in drinking water at sub- $\mu g/L$  (ppb) to low-to-mid- $\mu g/L$  levels. Currently, there are over 700 DBPs reported in drinking water, and new DBPs continue to be discovered. 1-3

Great knowledge gaps exist for toxicological information and health impacts of DBPs. Humans are exposed to DBPs through multiple routes, including ingestion (the common route studied), inhalation, and dermal exposures.3 Literature review indicates that only approximately 15% (~100) of identified DBPs have been assessed with in vitro bioassays and a few with chronic in vivo studies.<sup>2-4</sup> Potential health risks of DBPs have been reported, including cancer and other adverse reproductive effects, such as early term miscarriage and birth defects. 5-7 An association of specific cancers and exposure to disinfected water has emerged by epidemiological research. 5,8,9 Several toxicity mechanisms for DBPs have been implicated, including genotoxicity, oxidative stress, disruption of folate metabolism, and cell cycle disruption. 5,8,9 Genotoxicity is of particular importance because of its link to mutagenicity, carcinogenicity, as well as cancer.<sup>7,10</sup>

The genotoxicity of evaluated DBPs seems to be dependent on their structure and substituents. For example, among the halogenated DBPs, iodinated DBPs were observed to be more toxic than their brominated and chlorinated analogues. 11,12 Nitrogen-containing DBPs were more genotoxic than the DBPs that do not contain nitrogen.<sup>3,13</sup> Genotoxicity mechanisms of DBPs are also strongly related to their structures. For example, for halogenated DBPs, oxidative stress-induced DNA damage<sup>14-21</sup> and DNA alkylation<sup>22-25</sup> are two major mechanisms. Halonitriles may also induce genomic damage by cell cycle

December 11, 2017 Received: Revised: April 9, 2018 Accepted: April 16, 2018 Published: April 16, 2018

Department of Civil and Environmental Engineering, Northeastern University, 360 Huntington Avenue, Boston, Massachusetts 02115, United States

<sup>&</sup>lt;sup>‡</sup>Institute of Materia Medica, Chinese Academy of Medical Sciences and Peking Union Medical College, Beijing, 100050, China §Safe Global Water Institute and Department of Crop Sciences, University of Illinois at Urbana—Champaign, Urbana, Illinois 61801, United States

School of Civil and Environmental Engineering, Cornell University, Ithaca, New York 14850, United States

Table 1. Summary of PELI-Based Molecular End Points (PELI<sub>max</sub>, PELI1.5, and Geno-TEQ1.5 (MMC as reference compound) with  $R^2$  Indicating the Fitness of the Data to Four Parameter Logistic Models (in Table S1) for 20 DBPs Tested in This Study and Phenotypic End Points from the Literature  $^{40,a}$ 

class	chemical	PELI1.5 (mM)	geno-TEQ1.5 (in reference to MMC)	Ames (mutants/ $\mu$ M) <sup>5,21,58,59</sup>	$_{(\mu M)^{5,12,b}}^{GP}$	TD <sub>50</sub> (mg kg <sup>-1</sup> day <sup>-1</sup> , mice) <sup>60</sup>	carcinogenicity <sup>5,60</sup>
HAAs/iodo-acids	chloroacetic acid	$8.826 \times 10^{-7}$	14.820	27	411	_	_
	bromoacetic acid	$4.028 \times 10^{-4}$	0.032	5465	17	NA	NA
	iodoacetic acid	$3.240 \times 10^{-5}$	0.404	14129	8.7	NA	NA
	trichloroacetic acid (TCA)	$4.123 \times 10^{-3}$	0.003	-	-	584	+
oxyhalides	sodium bromate	$5.451 \times 10^{-6}$	2.400	_	NA	41	+
	sodium chlorite	$1.648 \times 10^{-6}$	7.937	26.5	NA	_	_
trihalomethanes (THMs)	bromodichloromethane	$5.245 \times 10^{-5}$	0.249	0.6254	_	47.7	+
	chlorodibromomethane	$3.254 \times 10^{-5}$	0.402	288.6	_	139	+
halonitromethanes	trichloronitromethane	$4.015 \times 10^{-7}$	32.578	40.5	93.4	_	_
nitrosamines	N-nitrosodimethylamine (NDMA)	$7.065 \times 10^{-8}$	185.138	533 <sup>c</sup>	220	0.189	+
haloamides	chloroacetamide	$2.071 \times 10^{-6}$	6.316	NA	1380	NA	NA
	2-bromoacetamide	$1.051 \times 10^{-6}$	12.445	NA	36.8	NA	NA
	2,2-dichloroacetamide	$1.703 \times 10^{-6}$	7.681	NA	_	NA	NA
halonitriles (HANs)	dichloroacetonitrile	$5.664 \times 10^{-7}$	23.093	+	2750	NA	NA
	dibromoacetonitrile	$7.155 \times 10^{-4}$	0.018	+	47.1	NA	+
	chloroacetonitrile	NA	NA	+	601	NA	+
	iodoacetonitrile	$2.384 \times 10^{-6}$	5.487	NA	37.1	NA	NA
aldehydes	trichloroacetaldehyde	$7.709 \times 10^{-6}$	1.697	+	_	99	+
	formaldehyde	$4.296 \times 10^{-6}$	3.045	+	NA	43.9	+
haloquinones	2,6-dichloro-1,4- benzoquinone	$7.259 \times 10^{-5}$	0.180	+	NA	NA	NA

<sup>a</sup>NA: PELI1.5 and geno-TEQ11.5 were not determined for chloroacetonitrile with PELI<sub>max</sub> less than 1.5 based on concentration response curve. <sup>b</sup>GP: the genotoxic potency derived from comet assay in CHO cells, which is the concentration at the midpoint of the concentration—response curve. <sup>5,12</sup> <sup>c</sup>CYP used in Ames test of *his* reversion for mutagenicity. <sup>61</sup>

disruption and the induction of hyperploidy.<sup>26</sup> Nitrosamines may act as alkylating agents after metabolism,<sup>27</sup> and formaldehyde can form DNA—protein cross-links.<sup>24</sup> The genotoxicity and mechanisms of most DBPs remain unknown.

The standard and most reliable genotoxicity tests are in vivo assays; however, they are resource-intensive and timeconsuming and therefore cannot meet the demand for evaluating a large number of potential genotoxic DBPs. 28,29 In vitro genotoxicity assays, including Ames, comet, and micronucleus tests, require relatively shorter testing time (several days) but often yield inconsistent or false results compared to in vivo outcomes 7,30,31 due to the inherent limitations of the target and DNA damage effects they can detect. 7,30 In recent years, high-throughput genotoxicity assessment has been reported where the activation of single or selected biomarkers indicative of DNA damage recognition and repair are used to indicate potential genotoxicity.<sup>7,3</sup> Our group has recently developed and validated a new quantitative toxicogenomics-based assay based on real time protein expression profiling of known DNA damage and repair pathways ensemble.<sup>38–41</sup> Compared to other biomarker-based tests, our assay derives quantitative end points that correlate with conventional genotoxicity end points and promises to be a cost-effective and mechanistic genotoxicity assessment assay.40,41

In this study, we employed the newly developed quantitative toxicogenomics genotoxicity assay to perform a mechanistic genotoxicity assessment and profiling of 20 DBPs representing nine different chemical classes of DBPs. The results provide new genotoxicity information and insights of underlying DNA damaging mechanisms at the molecular level for these 20 DBPs.

The high-resolution protein expression profiles of DNA damage and repair pathways also enabled DBP classification and further exploration of association between DBP chemical structure and the genotoxicity mechanisms.

#### ■ MATERIALS AND METHODS

**Chemicals.** Twenty DBPs were selected that belong to nine different chemical classes (Table 1, manufacturer information in Table S1). Each DBP was evaluated across a 6-log subcytotoxic concentration range (Table S1). The maximum noncytotoxic concentration was predetermined (>95% cell survival tested by growth inhibition in yeast for 24 h, Figure S1).

Yeast Whole Cell Array and Real Time Protein Expression Analysis upon DBP Exposure. The whole cell assay library consists of 38 in-frame GFP fusion proteins (Table S2) of Saccharomyces cerevisiae (Invitrogen, no. 95702, ATCC 201388) constructed by oligonucleotide-directed homologous recombination to tag each open reading frame (ORF) with Aequrea victoria GFP (S65T) in its chromosomal location at the 3' end, 42 covering all seven known DNA damage repair pathways. The library expresses full-length, chromosomally tagged green fluorescent protein fusion proteins, 42 which makes the GFP signal reflect protein expression directly.

Details of the proteomics assay for using GFP-tagged yeast cells were described in our previous reports.  $^{38-41}$  Briefly, the yeast strains were grown in clear bottom black 384-well plates (Costar) with Synthetic Dextrose base (SD medium) that contains –His Dropout (DO) supplement (Clontech, CA, US) for 4–6 h at 30 °C to reach early exponential growth. Then, 10  $\mu$ L DBP sample aliquots in PBS or vehicle control (PBS only) were added to each well to obtain the target

concentrations (Table S1). The plates were then placed in a Microplate Reader (Synergy H1Multi-Mode, Biotech, Winooski, VT) for absorbance (OD600 for cell growth), and GFP signal (filters with 485 nm excitation and 535 nm emission for protein expression) measurements were taken every 5 min for 2 h after double orbital shaking (425 cpm) for 1 min. All tests were performed in the dark in triplicate. Considering that all of the DBPs were tested at concentrations much lower than their solubility, evaporation and loss of the volatile DBPs during the 2 h assay was not considered in this study. 43,44

Protein Expression Profiling Data Processing and Quantitative Molecular End Point Derivation. Temporal protein expression profiling data of the yeast library were processed as described previously. Temporal OD and GFP raw data are first corrected by background OD and GFP signal of blank medium control with or without chemical. The protein expression level P for each protein biomarker (ORF) i, in treatment x, and at time point t is normalized by cell density as

$$P_{i,x,t} = \frac{\text{GFP}_{i,x,t\text{-corrected}}}{\text{OD}_{i,x,t\text{-corrected}}}$$
(1)

where  $GFP_{i,x,t\text{-corrected}}$  is the GFP reading of protein i in treatment x at time t corrected by the GFP reading in the blank medium control at time t;  $OD_{i,x,t\text{-corrected}}$  is the OD reading of protein i in treatment x at time t corrected by the OD reading in the blank medium control at time t.

The altered protein expression in relative to untreated control (without chemical) for a given protein ORFi in treatment x at time t due to chemical exposure, also referred as induction factor I, is calculated as

$$I_{i,x,t} = \frac{P_{i,x,t}}{P_{i,\text{untreated},t}} \tag{2}$$

where  $P_{i,x,t} = (GFP_{corrected}/OD_{corrected})_{treatment,x}$  is the altered protein expression GFP level for protein (ORF) i for treatment x at time t in the treated experimental condition with chemical exposure;  $P_{i,untreated,t} = (GFP_{corrected}/OD_{corrected})_{untreated control}$  is the altered protein expression GFP level for protein (ORF) i for treatment x at time t in the untreated control without chemical exposure. P values of both treated experiments and untreated controls are normalized and scaled against internal control (housekeeping protein PGK1<sup>46</sup>).

For the chemical-induced protein expression level changes of a treatment to be quantified, the protein effect level index (PELI) was derived as a quantitative molecular end point. The accumulative altered protein expression change over the 2 h exposure period for a given protein (ORF) i was calculated as

$$PELI_{ORF,i} = \frac{\int_{t=0}^{t} I_{upregulated} dt}{exposure time}$$
(3)

where t is the exposure time. For upregulated protein,  $I_{\rm upregulated} = I$ , when  $I \geq 1$ ; for proteins that showed downregulation,  $I_{\rm upregulated} = 1$  when I < 1.

The pathway activation response is calculated by integrating the protein expression changes for all of the proteins (ORFs) in a pathway as

$$PELI_{pathway j} = \frac{\sum_{i=1}^{n} w_i \times PELI_{ORFi}}{n}$$
(4)

where n is the number of ORFs in one particular pathway, and  $w_i$  is the weight factor of ORF<sub>i</sub>. For this study, we assigned a value of 1 for all of the weight factors.

Similar to  $PELI_{pathway}$ , the overall protein expression effect level for the DNA damage and repair pathway ensemble is calculated as  $PELI_{geno}$  with all of the  $PELI_{pathway}$  in the pathway ensemble library as

$$PELI_{geno} = \frac{\sum_{j=1}^{N} W_j \times PELI_{pathway j}}{N}$$
 (5)

where N is the number of pathways in this geno-sensor library,  $W_j$  is the weight factor of pathway j, and the value is assigned as 1 for this study.

For each DBP, six PELI<sub>geno</sub> values are evaluated by mean  $\pm$  SD. The PELI<sub>geno</sub>-based concentration—response pattern was modeled using a four parameter logistic (4PL) nonlinear regression model (the fitted curves). End point PELI<sub>max</sub> was derived based on the PELI<sub>geno</sub> concentration—response curve using 4PL model fitting. End point PELI1.5 was derived based on the concentration—response curves, which was defined as the corresponding concentration that causes the PELI value to reach 1.5, similar to the approach that has been applied for the *umuC* genotoxicity assay by Escher et al. and our previous study. Additionally, genotoxicity for each chemical with PELI1.5 was also expressed as toxic equivalents as

geno-TEQ1.5 = 
$$\frac{\text{PELI1.5}_{\text{reference compound}}}{\text{PELI1.5}_{\text{sample}}}$$
(6)

where mytomycin C (MMC) is used as reference compound.  $^{50}$  PELI1.5<sub>MMC</sub> = 2.15 ×  $10^{-3}$  mM based on our previous study.  $^{40,41}$ 

DNA Damage Alkaline Comet Assay in Human A549 Cells for Phenotypic Confirmation. The alkaline comet assay in human A549 cells <sup>51–53</sup> upon exposure to the DBPs at selected concentrations (details in Table S1) or 1% FBS-F12 medium only (as untreated control) for 24 h was carried out using Trevigen Inc. CometAssay 96 slides (www.trevigen.com). All the procedures were performed in the dark in triplicate. Each treatment (25 cells) was measured by the software CASP (University of Wroclaw, Institute of Theoretical Physics) randomly, and the damage was valued as % tail DNA (mean ± SD).<sup>12</sup>

Physicochemical Descriptors. Quantitative structure activity relationship (QSAR) analyses were performed to obtain insights into the physiochemical characteristics of DBPs that impact their genotoxicity. Various descriptors are used (Table S3) to support the QSAR analyses and they include the PaDEL descriptor software used for topological descriptors such as autocorrelation descriptors AATSC4c and AATSC3v, electrotopological state atom-type descriptor minsCl, and extended topochemical atom descriptor ETA Eta L.  $^{54}$  The US-EPA EPI suite was used for log  $K_{ow}$ ; Gaussian03 (using Hartree-Fock 3-21G) was used to calculate quantum chemical descriptors such as  $E_{\text{homo}}$  (the energy of the highest occupied molecular orbital),  $E_{lumo}$  (the energy of the lowest unoccupied molecular orbital), and G (Gibbs free energy), and the numbers of freely rotatable bonds, H acceptors, and H donors, polar surface area, and molecular weight were collected from the PubChem Web site (http:// www.ncbi.nlm.nih.gov/pccompound).

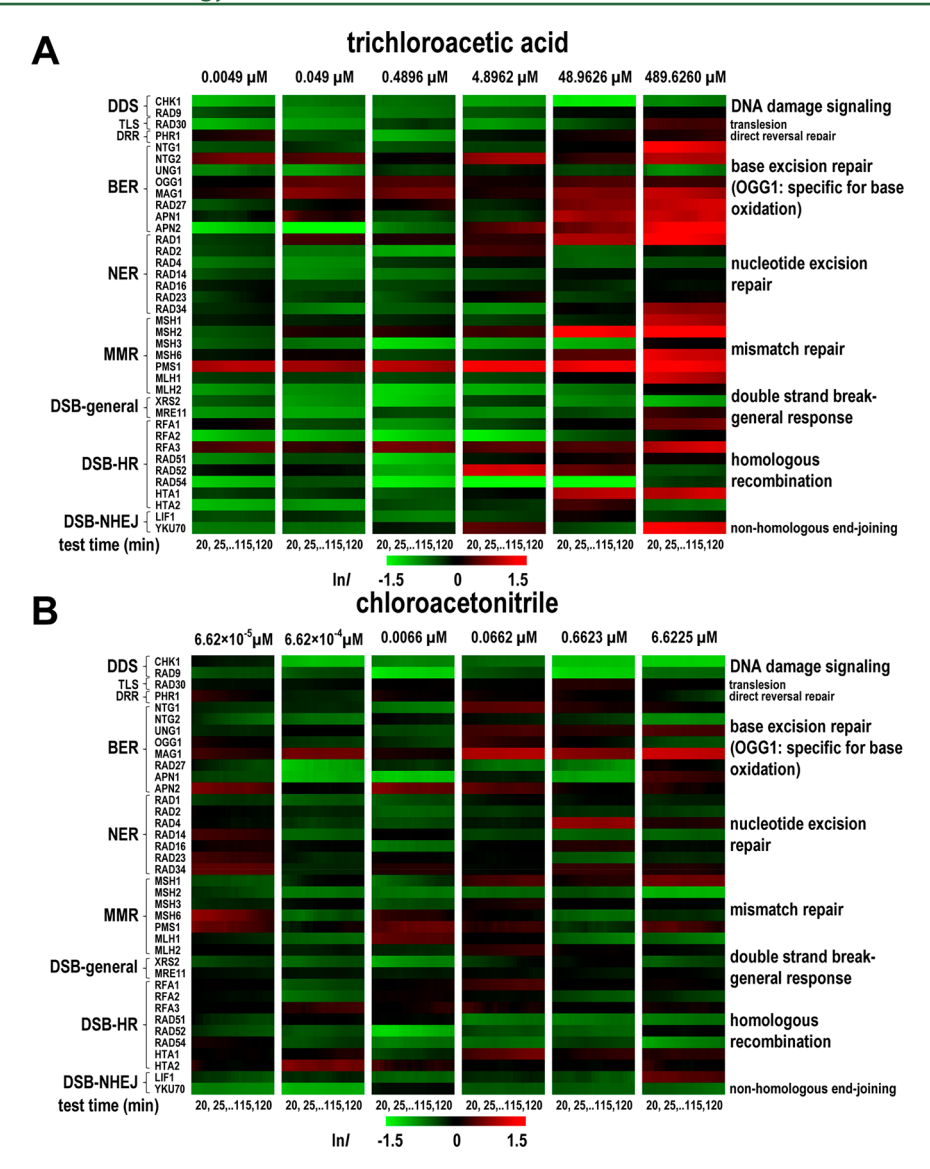


Figure 1. Temporal protein expression profiles of 38 biomarkers indicative of different DNA damage repair pathways upon exposure to trichloroacetic acid (A, a) haloacetic acid (A, a) and chloroacetonitrile (B, a) halonitrile) across six concentrations. The mean natural log of the induction factor (B, a) indicates the magnitude of altered protein expression (represented by a green-black-red color scale at the bottom. The red spectrum colors indicate upregulation, and the green spectrum colors indicate downregulation. Values beyond  $\pm 1.5$  are shown as  $\pm 1.5$ . X-axis top: concentrations for each chemical; X-axis bottom: testing time in minutes. The first data point shown is at 20 min after exposure due to data smoothing with moving average of every five data points. Y-axis left: clusters of proteins by DNA damage repair pathways and list of proteins (ORFs) tested; Y-axis right: description of DNA damage repair pathway abbreviations.

**Clustering Analysis.** Hierarchical clustering (HCL) was performed to cluster all 20 DBPs across six concentrations (120 samples in total) based on their protein expression profiles by software suit MeV (MutiExperiment Viewer) v4.8. The relationships were elucidated using the order of average linkage clustering based on Pearson correlation.

#### RESULTS AND DISCUSSION

DNA Damage Mechanisms Revealed by Concentration-Dependent, Chemical-Specific Temporal Differential Protein Expression Profiles among DBPs. The temporal altered protein expression profiles (Figure 1 and Figure S2) indicative of DNA damage and repair pathway activities were distinctive for each of the 20 DBPs tested in this study, suggesting compound-specific cellular responses resulted from their different DNA-damaging mechanisms. These

chemical-specific response patterns were also concentration-dependent, showing generally an increase in magnitude of altered protein expression as concentration increases (Figure 1A). For some DBPs tested, such as bromoacetic acid and dibromoacetonitrile (Figure S2), the highest exposure concentration led to decreases in the magnitude of upregulation or even a shift from up- to downregulation for most of the tested proteins. Consistent with our previous reports, <sup>38,40</sup> this was likely caused by the transition from a mode-of-action specific effect to subcytotoxic nonspecific cellular responses.

Correlation between Molecular End Points and Conventional Genotoxicity/Carcinogenicity End Points. The molecular quantifier  $PELI_{geno}$  exhibited a concentration response for all 20 DBPs tested (Figure 2). Our previous studies have demonstrated that quantitative genotoxicity molecular end point  $PELI_{geno}$  derived from the yeast assay

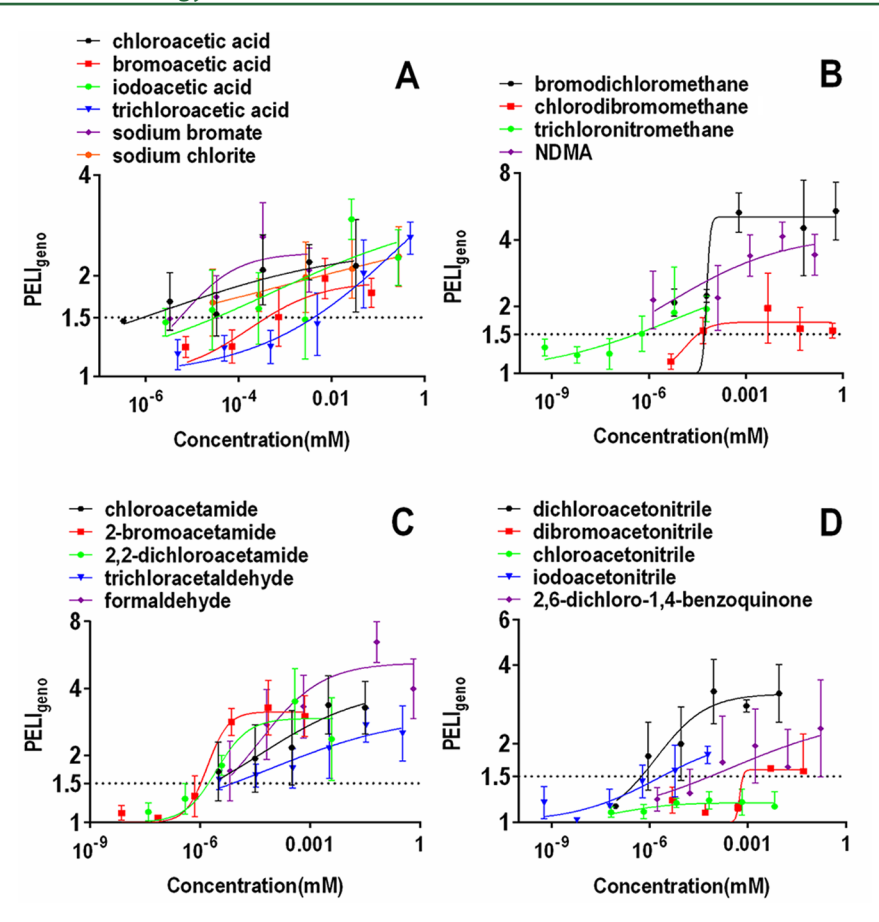
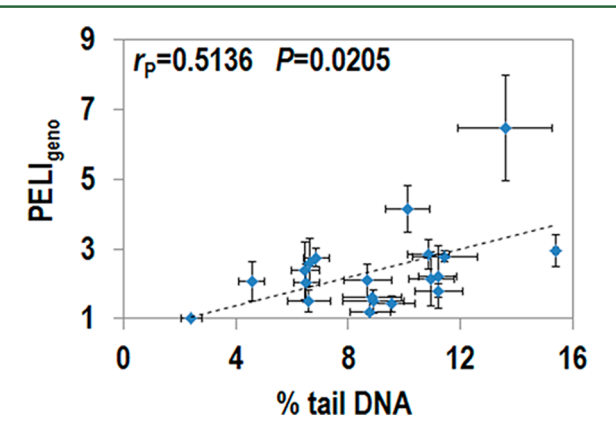


Figure 2. Concentration—response curves of the 20 DBPs tested based on PELI<sub>geno</sub> values: (A) haloacetic acids/iodo-acids and oxyhalides; (B) trihalomethanes, halonitromethanes, and NDMA; (C) haloamides and aldehydes; (D) halonitriles and 2,6-dichloro-1,4-benzoquinone. Data points with an error bar represent the PELI<sub>geno</sub> value determined at each concentration.  $R^2$  values indicative of fitness are listed in Table S1. Genotoxicity positive is defined as having a PELI<sub>max</sub> value (determined via model fitting concentration—response curves) greater than 1.5 (the dashed line).  $^{40}$  X-axis: concentration for chemicals studied (mM). Y-axis: PELI<sub>geno</sub>. Mean  $\pm$  SD, n=3. Note that data for five DBPs (trichloroacetic acid, NDMA, bromodichloromethane, chlorodibromomethane, and formaldehyde) were reported previously.

could statistically correlate to conventionally accepted genotoxicity assays for genotoxins, known genotoxic positive and negative chemicals. Consistent with previous studies, a statistically significant strong correlation ( $r_{\rm P}=0.5136,\ P=0.0205$ ) was observed between molecular genotoxicity end point PELI<sub>geno</sub> and the phenotpyic DNA damage end point % tail DNA from comet assay we performed in human A549 cells (Figure 3, comet assay details in Figure S3).

We also compared our quantitative genotoxicity molecular end point PELI1.5 with end points from different conventional genotoxicity assays (Table 1). We examined the correlation between the derived molecular end point PELI1.5 with other in vitro genotoxicity assay results including Ames assay in bacteria and comet assay in CHO cells. The results indicated that the molecular end point PELI1.5 correlated with both genotoxic potency (GP) of comet assay (CHO cell,  $r_{\rm P}=-0.5568$ , P=0.0945, n=10 in Figure 4A) and TD50 in vivo for carcinogenic potency (mice,  $r_{\rm P}=0.8186$ , P=0.0464, n=6 in Figure 4B). No significant correlation was found between yeast genotoxicity end points and Ames test (*his* reversion),  $r_{\rm P}=0.4472$ , P=0.2666, n=8; data not shown).

These results confirmed that our assay, consisting of biomarkers-ensemble indicative of DNA damage and repair pathway activities, could capture various DNA damage potentials and therefore reliably predict DNA damage-related carcinogenicity. The results also indicate the conservation of



**Figure 3.** Correlation of molecular end point PELI<sub>geno</sub> derived from our GFP-fused yeast assay with phenotypic end point of DNA damage measured by % tail DNA tested by alkaline comet assay in human A549 cell line for selected concentrations (Table S1). *X*-axis: 24 h DNA damage measured by % tail DNA in human A549 cells (details in Figure S3); *Y*-axis: PELI<sub>geno</sub>, the integrated quantifier of altered protein expression levels of 38 protein biomarkers indicative of DNA damage repair responses. Mean  $\pm$  SD, n=3.  $r_{\rm P}$  indicates the Pearson correlation coefficient of PELI<sub>geno</sub> to DNA damage comet assay phenotypic end points (% tail DNA).

DNA repair response among species. The quantitative correlation between the toxicogenomic assay-derived end

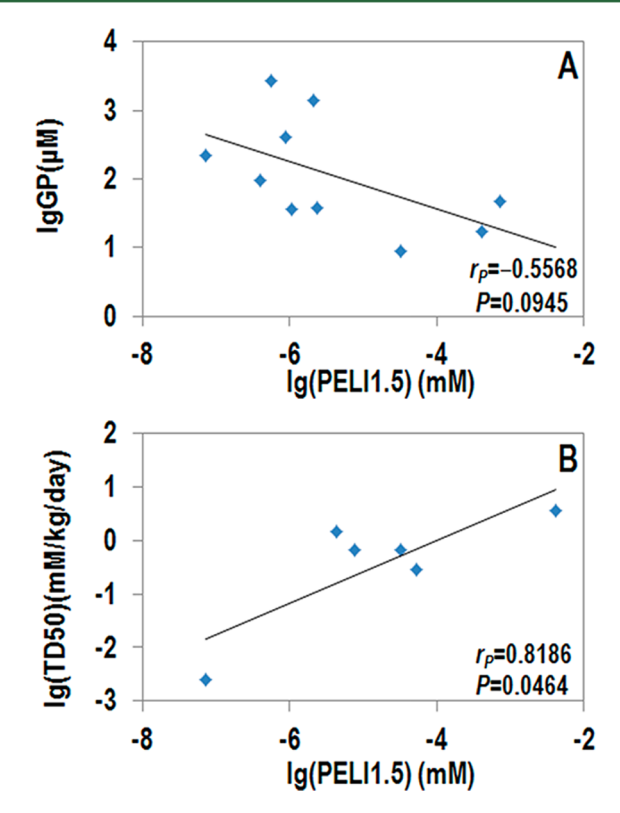


**Figure 4.** Correlation of molecular end point PELI1.5 with phenotypic end points: genotoxic potency from comet assay in CHO cells (A, n = 10) and carcinogenic potency from a 2-year carcinogenesis test in mice (B, n = 6) (data collected from references as shown in Table 1). *X*-axis: PELI1.5 determined via model fitting concentration—response curves (lg(PELI1.5), mM); *Y*-axis: genotoxic potency (lg(GP),  $\mu$ M, A) and carcinogenic potency (lg(TD<sub>50</sub>), mM kg<sup>-1</sup> day<sup>-1</sup>, B).  $r_{\rm P}$  indicates the Pearson correlation coefficient of PELI1.5 to phenotypic end points.

points and conventional end points suggest that it can possibly be incorporated into a toxicity and risk assessment framework. Our results are in general agreement with results from different genotoxicity assays reported in the literarure. Where inconsistencies were noted, these could be attributed to varying detection targets and inherent limitations of each specific assay as discussed previously.<sup>40</sup>

Note that although no extra metabolic activation (e.g., liver extract S9) was used for genotoxicity evaluation of DBPs in this study, detectable molecular genotoxicity was observed for the known metabolically activated genotoxicant NDMA.<sup>27</sup> Several cytochrome P-448 monooxygenase enzymes in yeast (including *S. cerevisiae* of this study) can perform Phase I metabolism on some compounds in a manner analogous to mammalian microsomal enzymes, although less efficiently.<sup>38,56,57</sup> The enzymatic capability of yeast may explain the genotoxicity observed in this study for NDMA without extra metabolic activation.

DNA Damaging Pathway Activation Profiling Revealed Distinct Genotoxicity Mechanisms among DBPs. As shown in Figure 5, the activation of biomarkers indicative of specific DNA damage and repair pathways revealed insights into the underlying mechanism(s) involved in the genotoxicity of studied DBPs; 40,41 16 out of 20 DBPs in this study induced oxidative DNA damage indicated by OGG1 upregulation (indicated by "oxidation" in Figure 5) of the base excision repair system (BER), which was consistent with their

strong oxidizing ability. 17,19,21,62 Activation of BER via other base damages, including base alkylation and deamination, as well as single strand break, was also widely observed for various DBPs at multiple concentrations, which is also consistent with their alkylating potential. 22,23 Strong activation of nucleotide excision repair (NER) was observed for NDMA and formaldehyde, which was consistent with the DNA single or double strand breaks caused by NDMA<sup>63</sup> and DNA-protein crosslinks led by formaldehyde,<sup>24</sup> respectively. The similarity of DNA damage repair pathway activation revealed by our assay to previously reported genotoxicity mechanisms suggest that the information obtained from our assay may provide insights into potential genotoxicity mechanisms of those DBPs that have not been well studied. For example, the pathway activation of oxidation in BER confirmed the oxidative damage effect of 2,6dichloro-1,4-benzoquinone, an emerging halobenzoquinone being studied in recent years. It was reported to induce cellular ROS, oxidative DNA adduct 8-OHdG, and activation of the Nrf2/ARE pathway (associated with oxidative stress) with an effect on intracellular antioxidant systems including GSH/ GSSG and antioxidant enzymes. 20,21,43,64

Examination and comparison of DNA damage and repair pathway activation profiles among DBPs suggest that genotoxicity of DBPs may be structure-dependent. For example, dichloroacetonitrile, dibromoacetonitrile, and two haloaldehydes analyzed in this study induced a wide range of pathway activations likely reflecting their strong oxidative damage to DNA structure. However, some DBPs within the same chemical class demonstrated different pathway activation patterns and magnitude. For example, chloroacetonitrile demonstrated little pathway activation compared to the other three halonitriles tested in this study. Our analyses revealed high-resolution molecular details of DNA damage effects of DBPs tested in this study.

Chemical Clustering of DBPs Based on DNA Damage Repair Pathway Protein Expression Profiles. The high-resolution molecular genotoxicity profiling of all known DNA damage repair pathways could serve as fingerprints for DBP clustering analysis and classification. We performed hierarchical clustering using average linkage clustering and Pearson correlation as shown in Figure 6. For most DBPs, the profiles of the same DBP at varying concentrations generally clustered together as a result of the chemical-specific DNA-damaging mechanism(s). However, some DBPs (e.g., formaldehyde and iodoacetonitrile) showed concentration-sensitive DNA-damaging profiles at varying concentrations.

The clustering analysis revealed clear clusters of DBPs that shared high similarity in their DNA damage effects profiles, such as the clusters of chloroacetamide and dichloroacetamide, formaldehyde and iodoacetic acid, and that of trichloroacetic acid (TCA) and chloroacetonitrile. The results indicated that DBPs from the same chemical structural class may not share similar genotoxicity mechanisms as often expected. For example, bromodichloromethane—chlorodibromomethane exhibited distant profiles and so were the two aldehydes (trichloroacetaldehyde—formaldehyde). Therefore, gene or protein profiling fingerprints provided by the toxicogenomics assay can better distinguish chemicals based on their molecular toxicity mechanisms.

QSAR Physicochemical Descriptors versus Genotoxicity to Assess Mechanisms. Quantitative structure—activity relationship (QSAR) has been employed as a diagnostic tool to assess the molecular initiating events of DBPs in the interaction

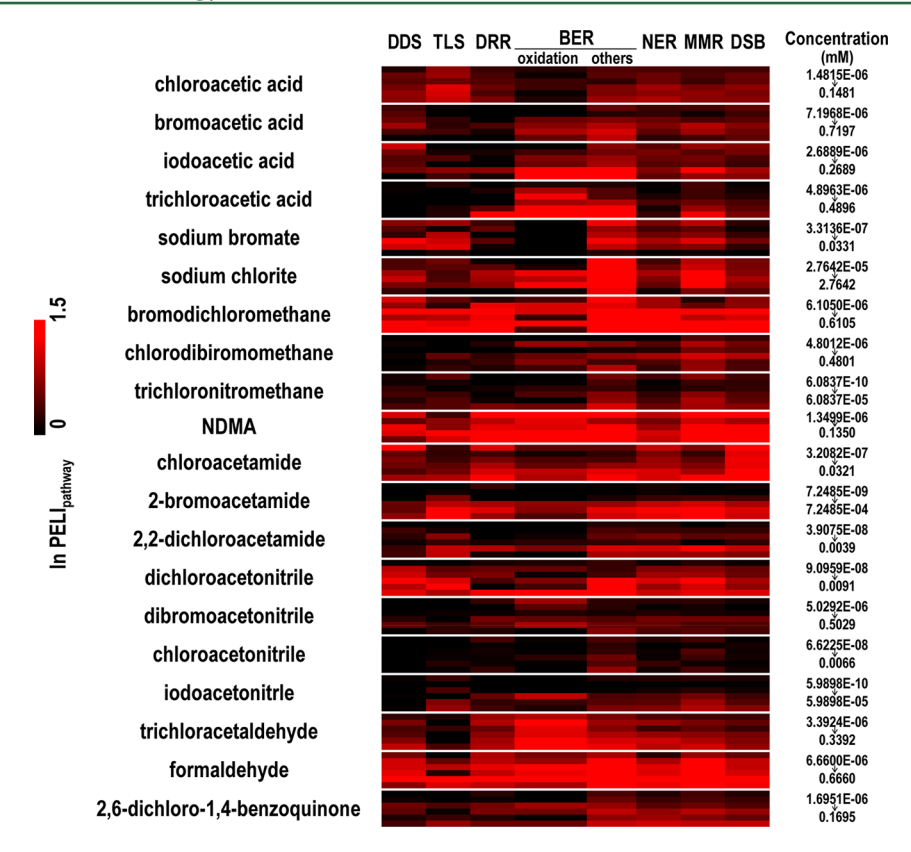


Figure 5. DNA damage repair pathway response profiles reveal distinct potential DNA damage mechanisms among different DBPs across 6-log concentrations (five DBPs were reported previously<sup>40</sup>). The mean natural log value of PELI<sub>pathway</sub> indicates the magnitude of pathway responses (represented by a black—red color scale at left; values over 1.5 are shown in the same color as 1.5). X-axis top: pathways of DNA damage repair (see Figure 1 and Table S2 for details). Y-axis left: DBPs tested in this study; Y-axis right: concentrations from lowest to highest from top to bottom (see concentrations in Table S1). Aberrations for DNA repair pathways: DDS, DNA damage signaling; TLS, translesion synthesis; DRR, direct reversal repair; BER, base excision repair; NER, nucleotide excision repair; MMR, mismatch repair; DSB, double strand break.

with DNA.4,65 Here, we explored the QSAR modeling for predicting molecular end points PELI<sub>max</sub> and PELI1.5. For different classes of DBPs, their genotoxicity mechanism(s) may be reflected by different physicochemical properties and thus may lead to different relationships with different descriptor(s). Although only a few DBPs were tested for each chemical class in this study, linear regression could still be useful to identify potential toxicity mechanism(s) (descriptors in Table 2, linear regression in Figure S4). For example, for the four HAAs, AATSC3v (an autocorrelation descriptor of average centered Broto-Moreau autocorrelation weighted by van der Waals volumes), and  $E_{lomo}$  (the energy of the lowest unoccupied molecular orbital) seemed to be suitable descriptors for PELI<sub>max</sub> modeling with  $R^2 = 0.9991$  (P = 0.0297). Log  $K_{ow}$ , and  $E_{lomo}$ could be used for their PELI1.5 prediction with  $R^2 = 0.9183$ (P=0.2858), suggesting that the electron-donating and -accepting ability (reflected by  $E_{\rm lomo}$ )<sup>66</sup> and topological property (reflected by AATSC3v) may correlate to HAA genotoxicity. For the four halonitriles tested, PELI<sub>max</sub> could be predicted by AATSC3v with  $R^2 = 0.7686$  (P = 0.1233), and PELI1.5 could be predicted by AATSC3v with  $R^2 = 0.9894$  (P = 0.1379), suggesting that the genotoxicity of halonitriles may be mainly related to their topological property. For the three haloamides tested, PELI<sub>max</sub> could be predicted by ATS3p (an autocorrelation descriptor of centered Broto-Moreau autocorrelation weighted by polarizabilities) with  $R^2 = 0.9345$  (P=0.1645), and PELI1.5 could be predicted by G (Gibbs free energy) with  $R^2$  = 0.9943 (P= 0.0482). The correlation of  $E_{lomo}$  to toxicity of

haloacetic acids is consistent with other published studies. 4,16,25,67

The QSAR modeling exercise of the DBPs suggested that chemical properties of the molecules, for example, topological and quantum chemical properties, correlate with the genotoxicity of DBPs. In addition, the correlation of different descriptors implicated different mechanism(s). For example, electron-donating and -accepting ability may be involved for DBPs in certain chemical classes.

In this study, we applied a quantitative toxicogenomics-based assay for relatively fast (2 h assay time length compared with days required as in the comet assay and micronucleus test), efficient, and mechanistic genotoxicity analyses for 20 DBPs in various chemical classes. The results provided new insights and fundamental knowledge of DNA-damage-related genotoxicity of studied DBPs and contributed to filling of the existing knowledge gap in DBP genotoxicity. PELI-based quantitative end points showed correlation with conventional genotoxicity and carcinogenicity end points and therefore can be potentially incorporated into DBP risk assessment. The pathway activation and clustering analysis based on the high-resolution protein expression profiles enabled DBP classification based on their molecular initiating patterns. The analyses also provide evidence for a structure-genotoxicity relationship of DBPs. Initial exploration of QSAR modeling using molecular genotoxicity end points (PELI) suggested that genotoxicity of DBPs in this study correlated with topological and quantum chemical descriptors. Establishment of such a unified DBP

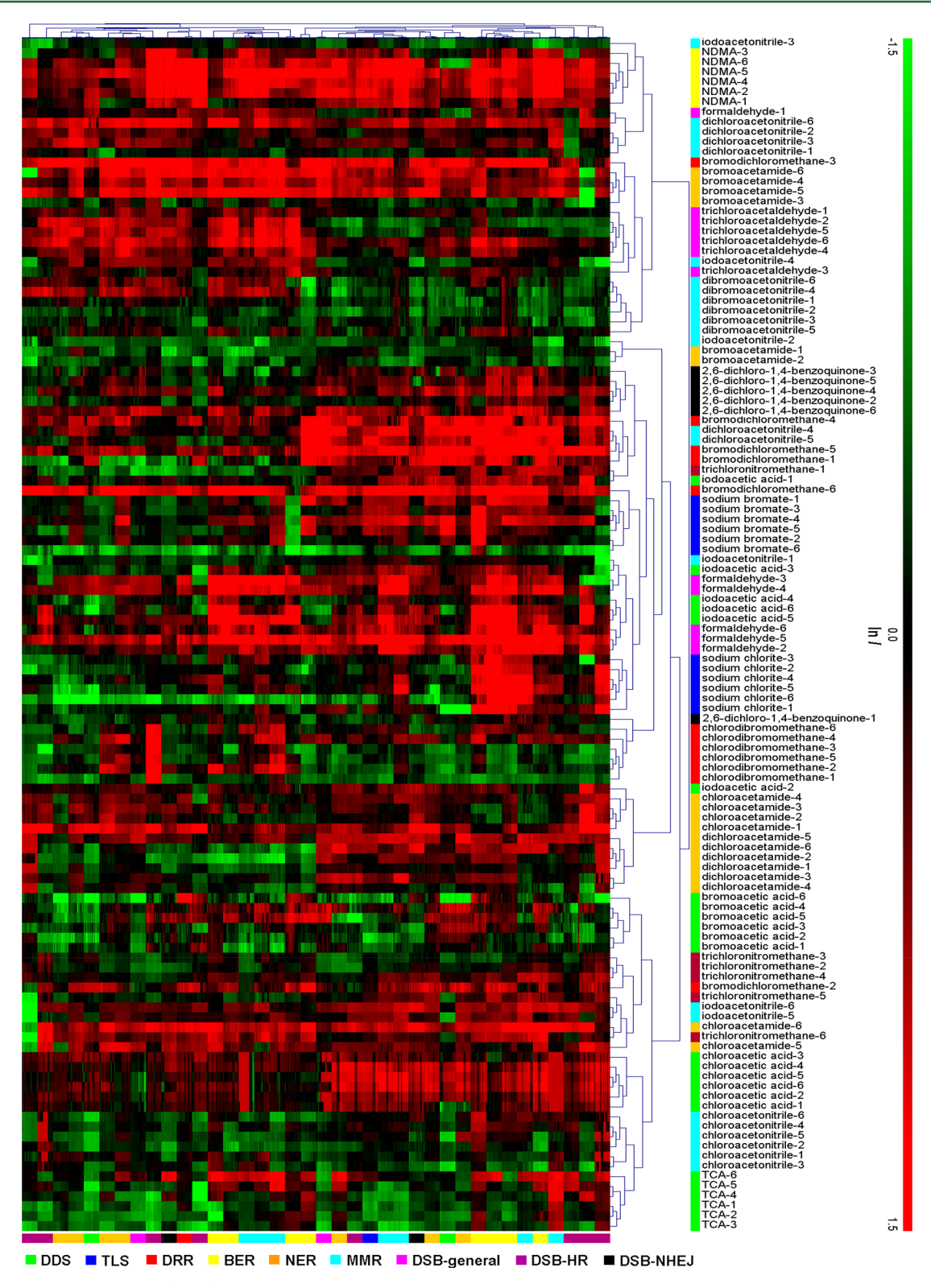


Figure 6. Hierarchical clustering (HCL) analysis diagram based on protein expression profiles of the 20 DBPs across six concentrations in this study (average linkage clustering, Pearson correlation). Rows represent individual experimental samples. Columns represent protein expression profiles. The mean magnitude of altered protein expression ( $\ln I$ ) is represented by a green-black-red color spectrum. Red spectrum colors indicate upregulation; green spectrum colors indicate downregulation. Values beyond  $\pm 1.5$  are shown in the same color as  $\pm 1.5$ . Numbers 1-6 represent concentrations from lowest to highest (see concentrations in Table S1). X-axis top: cluster roots of protein biomarkers used in this study; X-axis bottom: DNA damage and repair pathways with color codes; Y-axis right: cluster roots and list of chemicals tested with color codes for chemical classes.

genotoxicity database will allow identification and prediction of genotoxicity and mechanism analysis for new DBPs in water samples. <sup>4</sup> The assay can be further applied to evaluate effects of the DBP mixtures as they present in drinking water. This study

Table 2. Results of the Correlation between PELI-based Endpoints and Physicochemical Descriptors

		PELI <sub>max</sub>	lg(PELI1.5)		
	descriptor(s)	$r (p value)^a$	descriptor(s)	r (p value)	
HAAs	$E_{ m lomo}$ AATSC3v	-0.9783 (0.0262) -0.4196 (0.5804)	$\logK_{ m ow} \ E_{ m lomo}$	0.7265 (0.2735) -0.6547 (0.3453)	
HANs haloamides	AATSC3v ATS3p	0.8767 (0.1233) -0.9667 (0.1648)	AATSC3v G	-0.9766 (0.1379) 0.9971 (0.0482)	

ar indicates the correlation for the single descriptor. The fitness of the regression of multiple descriptors is shown in Figure S4.

demonstrated that the quantitative toxicogenomics-based genotoxicity assay can serve as an alternative and complementary method for genotoxicity screening and evaluation of environmental water pollutants such as DBPs and provide timely guidance for drinking water safety and public health research.

### ASSOCIATED CONTENT

# S Supporting Information

The Supporting Information is available free of charge on the ACS Publications website at DOI: 10.1021/acs.est.7b06389.

Details for the 20 DBPs and their concentration range in the study, 24 h cytotoxicity of chemicals in yeast cells for concentration range selection, yeast library used in this study, physicochemical descriptors of the 20 DBPs in this study, real-time protein expression profiles of all other 18 DBPs tested and mitomycin C as reference compound in this study, results of the Comet assay in human A549 cells, and linear regression of physicochemical descriptors for the mechanistic study (PDF)

#### AUTHOR INFORMATION

# Corresponding Author

\*E-mail: aprilgu@cornell.edu.

#### ORCID

Sheikh Mokhlesur Rahman: 0000-0002-3174-856X

Micheal J. Plewa: 0000-0001-8307-1629 April Z. Gu: 0000-0002-5099-5531

#### **Notes**

The authors declare no competing financial interest.

## ACKNOWLEDGMENTS

This study was supported by the United States National Science Foundation (NSF, CBET-1437257, CBET-1810769, IIS-1546428), National Institute of Environmental Health Sciences (NIEHS, PROTECT 3P42ES017109, and CRECE 1P50ES026049), and Environmental Protection Agency (EPA, CRECE 83615501).

# REFERENCES

- (1) Richardson, S. D.; Postigo, C. Formation of DBPs: state of the science. In *Recent Advances in Disinfection By-Products*; Karanfil, T., Mitch, B., Westerhoff, P., Xie, Y., Eds.; ACS Publications: Washington, DC, 2015; pp 189–214.
- (2) Plewa, M. J.; Richardson, S. D. Disinfection By-Products in Drinking Water, Recycled Water and Wastewater: Formation, Detection, Toxicity and Health Effects: Preface. *J. Environ. Sci.* **2017**, 58 (Supplement C), 1.
- (3) Richardson, S.; Postigo, C. Drinking water disinfection by-products 2012, 1-45.

- (4) Stalter, D.; O'Malley, E.; von Gunten, U.; Escher, B. I. Fingerprinting the reactive toxicity pathways of 50 drinking water disinfection by-products. *Water Res.* **2016**, *91*, 19–30.
- (5) Richardson, S. D.; Plewa, M. J.; Wagner, E. D.; Schoeny, R.; DeMarini, D. M. Occurrence, genotoxicity, and carcinogenicity of regulated and emerging disinfection by-products in drinking water: A review and roadmap for research. *Mutat. Res., Rev. Mutat. Res.* **2007**, 636 (1–3), 178–242.
- (6) Singh, N.; Manshian, B.; Jenkins, G. J. S.; Griffiths, S. M.; Williams, P. M.; Maffeis, T. G. G.; Wright, C. J.; Doak, S. H. NanoGenotoxicology: The DNA damaging potential of engineered nanomaterials. *Biomaterials* **2009**, *30* (23–24), 3891–3914.
- (7) Ahn, J. M.; Hwang, E. T.; Youn, C. H.; Banu, D. L.; Kim, B. C.; Niazi, J. H.; Gu, M. B. Prediction and classification of the modes of genotoxic actions using bacterial biosensors specific for DNA damages. *Biosens. Bioelectron.* **2009**, *25* (4), 767–772.
- (8) Bull, R. J.; Reckhow, D. A.; Rotello, V.; Bull, O. M.; Kim, J. *Use of toxicological and chemical models to prioritize DBP research*; American Water Works Association: Denver, CO, 2006.
- (9) Nieuwenhuijsen, M. J.; Grellier, J.; Smith, R.; Iszatt, N.; Bennett, J.; Best, N.; Toledano, M. The epidemiology and possible mechanisms of disinfection by-products in drinking water. *Philos. Trans. R. Soc., A* **2009**, *367* (1904), 4043–76.
- (10) Reifferscheid, G.; Buchinger, S. Cell-Based Genotoxicity Testing. In Whole Cell Sensing System II; Springer, 2009; pp 85–111.
- (11) Plewa, M. J.; Wagner, E. D.; Richardson, S. D.; Thruston, A. D.; Woo, Y.-T.; McKague, A. B. Chemical and biological characterization of newly discovered iodoacid drinking water disinfection byproducts. *Environ. Sci. Technol.* **2004**, *38* (18), 4713–4722.
- (12) Plewa, M. J.; Wagner, E. D. Mammalian Cell Cytotoxicity and Genotoxicity of Disinfection By-Products; Water Research Foundation, 2009.
- (13) Plewa, M. J.; Wagner, E. D.; Muellner, M. G.; Hsu, K.-M.; Richardson, S. D. Comparative mammalian cell toxicity of N-DBPs and C-DBPs. In *Occurrence, Formation, Health Effects and Control of Disinfection By-Products in Drinking Water*; Karanfil, T., Krasner, S. W., Westerhoff, P., Xie, Y., Eds.; ACS Publications: Washington, D.C, 2008; Vol. 995, pp 36–50.
- (14) Pals, J. A.; Ang, J. K.; Wagner, E. D.; Plewa, M. J. Biological mechanism for the toxicity of haloacetic acid drinking water disinfection byproducts. *Environ. Sci. Technol.* **2011**, 45 (13), 5791–5797.
- (15) Dad, A.; Jeong, C. H.; Pals, J. A.; Wagner, E. D.; Plewa, M. J. Pyruvate remediation of cell stress and genotoxicity induced by haloacetic acid drinking water disinfection by-products. *Environmental and molecular mutagenesis* **2013**, 54 (8), 629–637.
- (16) Pals, J.; Attene-Ramos, M. S.; Xia, M.; Wagner, E. D.; Plewa, M. J. Human cell toxicogenomic analysis linking reactive oxygen species to the toxicity of monohaloacetic acid drinking water disinfection byproducts. *Environ. Sci. Technol.* **2013**, *47* (21), 12514–12523.
- (17) Liviac, D.; Creus, A.; Marcos, R. Genotoxicity analysis of two halonitromethanes, a novel group of disinfection by-products (DBPs), in human cells treated in vitro. *Environ. Res.* **2009**, *109* (3), 232–238.
- (18) Plewa, M. J.; Wagner, E. D.; Jazwierska, P.; Richardson, S. D.; Chen, P. H.; McKague, A. B. Halonitromethane drinking water disinfection byproducts: chemical characterization and mammalian cell cytotoxicity and genotoxicity. *Environ. Sci. Technol.* **2004**, *38* (1), 62–68.

- (19) Ballmaier, D.; Epe, B. DNA damage by bromate: mechanism and consequences. *Toxicology* **2006**, *221* (2), 166–171.
- (20) Procházka, E.; Escher, B. I.; Plewa, M. J.; Leusch, F. D. In vitro cytotoxicity and adaptive stress responses to selected haloacetic acid and halobenzoquinone water disinfection byproducts. *Chem. Res. Toxicol.* **2015**, 28 (10), 2059–2068.
- (21) Li, J.; Wang, W.; Moe, B.; Wang, H.; Li, X.-F. Chemical and Toxicological Characterization of Halobenzoquinones, an Emerging Class of Disinfection Byproducts. *Chem. Res. Toxicol.* **2015**, 28 (3), 306–318.
- (22) Daniel, F. B.; Schenck, K. M.; Mattox, J. K.; Lin, E. L.; Haas, D. L.; Pereira, M. A. Genotoxic properties of haloacetonitriles: drinking water by-products of chlorine disinfection. *Toxicol. Sci.* **1986**, *6* (3), 447–53.
- (23) Muellner, M. G.; Wagner, E. D.; McCalla, K.; Richardson, S. D.; Woo, Y. T.; Plewa, M. J. Haloacetonitriles vs. regulated haloacetic acids: are nitrogen-containing DBPs more toxic? *Environ. Sci. Technol.* **2007**, *41* (2), 645–51.
- (24) Vock, E.; Lutz, W.; Ilinskaya, O.; Vamvakas, S. Discrimination between genotoxicity and cytotoxicity for the induction of DNA double-strand breaks in cells treated with aldehydes and diepoxides. *Mutat. Res., Genet. Toxicol. Environ. Mutagen.* 1999, 441 (1), 85–93.
- (25) Pals, J. A.; Wagner, E. D.; Plewa, M. J. Energy of the Lowest Unoccupied Molecular Orbital, Thiol Reactivity, and Toxicity of Three Monobrominated Water Disinfection Byproducts. *Environ. Sci. Technol.* **2016**, *50* (6), 3215–3221.
- (26) Komaki, Y.; Mariñas, B. J.; Plewa, M. J. Toxicity of drinking water disinfection byproducts: cell cycle alterations induced by the monohaloacetonitriles. *Environ. Sci. Technol.* **2014**, *48* (19), 11662–11669
- (27) Swenberg, J. A.; Hoel, D. G.; Magee, P. N. Mechanistic and statistical insight into the large carcinogenesis bioassays on N-nitrosodiethylamine and N-nitrosodimethylamine. *Cancer Res.* **1991**, *51* (23 Part 2), 6409–6414.
- (28) Shukla, S. J.; Huang, R.; Austin, C. P.; Xia, M. The future of toxicity testing: a focus on in vitro methods using a quantitative high-throughput screening platform. *Drug Discovery Today* **2010**, *15* (23–24), 997–1007.
- (29) Johnson, T. D. Report calls for examination of chemical safety: National coalition notes difficulty determining exposures. *Nation's Health* **2011**, *41* (6), 9–9.
- (30) Knight, A. W.; Little, S.; Houck, K.; Dix, D.; Judson, R.; Richard, A.; McCarroll, N.; Akerman, G.; Yang, C.; Birrell, L. Evaluation of high-throughput genotoxicity assays used in profiling the US EPA ToxCast chemicals. *Regul. Toxicol. Pharmacol.* **2009**, *55* (2), 188–199.
- (31) Walmsley, R. M.; Billinton, N. How accurate is in vitro prediction of carcinogenicity? *British journal of pharmacology* **2011**, 162 (6), 1250–1258.
- (32) Muellner, M. G.; Attene-Ramos, M. S.; Hudson, M. E.; Wagner, E. D.; Plewa, M. J. Human cell toxicogenomic analysis of bromoacetic acid: A regulated drinking water disinfection by-product. *Environ. Mol. Mutagen.* **2010**, *51* (3), 205–214.
- (33) Attene-Ramos, M. S.; Wagner, E. D.; Plewa, M. J. Comparative human cell toxicogenomic analysis of monohaloacetic acid drinking water disinfection byproducts. *Environ. Sci. Technol.* **2010**, *44* (19), 7206–7212.
- (34) Mahadevan, B.; Snyder, R. D.; Waters, M. D.; Benz, R. D.; Kemper, R. A.; Tice, R. R.; Richard, A. M. Genetic Toxicology in the 21st Century: Reflections and Future Directions. *Environmental and molecular mutagenesis* **2011**, *52* (5), 339–354.
- (35) Walmsley, R.; Billinton, N.; Heyer, W. Green fluorescent protein as a reporter for the DNA damage-induced gene RAD54 in Saccharomyces cerevisiae. *Yeast* 1997, 13 (16), 1535–1545.
- (36) Cahill, P.; Knight, A.; Billinton, N.; Barker, M.; Walsh, L.; Keenan, P.; Williams, C.; Tweats, D.; Walmsley, R. The Green-Screen® genotoxicity assay: a screening validation programme. *Mutagenesis* **2004**, *19* (2), 105–119.
- (37) Attene-Ramos, M. S.; Huang, R.; Sam, M.; Witt, K. L.; Richard, A.; Tice, R. R.; Simeonov, A.; Austin, C. P.; Xia, M. Profiling of the

- Tox21 chemical collection for mitochondrial function to identify compounds that acutely decrease mitochondrial membrane potential. *Environmental Health Perspectives (Online)* **2015**, 123 (1), 49.
- (38) O'Connor, S. T. F.; Lan, J.; North, M.; Loguinov, A.; Zhang, L.; Smith, M. T.; Gu, A. Z.; Vulpe, C. Genome-wide functional and stress response profiling reveals toxic mechanism and genes required for tolerance to benzo [a] pyrene in S. cerevisiae. *Front. Genet.* **2013**, 3, 316.
- (39) Lan, J.; Hu, M.; Gao, C.; Alshawabkeh, A.; Gu, A. Z. Toxicity Assessment of 4-Methyl-1-cyclohexanemethanol and Its Metabolites in Response to a Recent Chemical Spill in West Virginia, USA. *Environ. Sci. Technol.* **2015**, 49 (10), 6284–6293.
- (40) Lan, J.; Gou, N.; Rahman, S. M.; Gao, C.; He, M.; Gu, A. Z. A quantitative toxicogenomics assay for high-throughput and mechanistic genotoxicity assessment and screening of environmental pollutants. *Environ. Sci. Technol.* **2016**, *50* (6), 3202–3214.
- (41) Lan, J.; Gou, N.; Gao, C.; He, M.; Gu, A. Comparative and Mechanistic Genotoxicity Assessment of Nanomaterials via A Quantitative Toxicogenomics Approach Across Multiple Species. *Environ. Sci. Technol.* **2014**, *48* (21), 12937–45.
- (42) Huh, W. K.; Falvo, J. V.; Gerke, L. C.; Carroll, A. S.; Howson, R. W.; Weissman, J. S.; O'Shea, E. K. Global analysis of protein localization in budding yeast. *Nature* **2003**, 425 (6959), 686–91.
- (43) Zuo, Y.-T.; Hu, Y.; Lu, W.-W.; Cao, J.-J.; Wang, F.; Han, X.; Lu, W.-Q.; Liu, A.-L. Toxicity of 2,6-dichloro-1,4-benzoquinone and five regulated drinking water disinfection by-products for the Caenorhabditis elegans nematode. *J. Hazard. Mater.* **2017**, 321, 456–463.
- (44) Zhang, S.; Miao, D.; Tan, L.; Liu, A.; Lu, W. Comparative cytotoxic and genotoxic potential of 13 drinking water disinfection by-products using a microplate-based cytotoxicity assay and a developed SOS/umu assay. *Mutagenesis* **2015**, *31* (1), 35–41.
- (45) O'Connor, S. T. F.; Lan, J.; North, M.; Loguinov, A.; Zhang, L.; Smith, M. T.; Gu, A. Z.; Vulpe, C. Genome-wide functional and stress response profiling reveals toxic mechanism and genes required for tolerance to benzo [a] pyrene in S. cerevisiae. *Front. Genet.* **2013**, *3*, 1.
- (46) Nakatani, Y.; Yamada, R.; Ogino, C.; Kondo, A. Synergetic effect of yeast cell-surface expression of cellulase and expansin-like protein on direct ethanol production from cellulose. *Microb. Cell Fact.* **2013**, 12 (1), 66.
- (47) Gou, N.; Gu, A. Z. A New Transcriptional Effect Level Index (TELI) for Toxicogenomics-based Toxicity Assessment. *Environ. Sci. Technol.* **2011**, 45 (12), 5410–5417.
- (48) Escher, B. I.; Bramaz, N.; Mueller, J. F.; Quayle, P.; Rutishauser, S.; Vermeirssen, E. L. Toxic equivalent concentrations (TEQs) for baseline toxicity and specific modes of action as a tool to improve interpretation of ecotoxicity testing of environmental samples. *J. Environ. Monit.* 2008, 10 (5), 612–21.
- (49) Gou, N.; Yuan, S.; Lan, J.; Gao, C.; Alshawabkeh, A. N.; Gu, A. Z. A quantitative toxicogenomics assay reveals the evolution and nature of toxicity during the transformation of environmental pollutants. *Environ. Sci. Technol.* **2014**, *48* (15), 8855–63.
- (50) Salamone, M.; Heddle, J.; Stuart, E.; Katz, M. Towards an improved micronucleus test Studies on 3 model agents, mitomycin C, cyclophosphamide and dimethylbenzanthracene. *Mutation Research/fundamental & Molecular Mechanisms of Mutagenesis* **1980**, 74 (5),
- (51) Weber, S.; Hebestreit, M.; Wilms, T.; Conroy, L. L.; Rodrigo, G. Comet assay and air—liquid interface exposure system: a new combination to evaluate genotoxic effects of cigarette whole smoke in human lung cell lines. *Toxicol. In Vitro* **2013**, *27* (6), 1987–1991.
- (52) Godschalk, R. W.; Ersson, C.; Riso, P.; Porrini, M.; Langie, S. A.; van Schooten, F.-J.; Azqueta, A.; Collins, A. R.; Jones, G. D.; Kwok, R. W. DNA-repair measurements by use of the modified comet assay: an inter-laboratory comparison within the European Comet Assay Validation Group (ECVAG). *Mutat. Res., Genet. Toxicol. Environ. Mutagen.* 2013, 757 (1), 60–67.
- (53) Bausinger, J.; Schütz, P.; Piberger, A. L.; Speit, G. Further characterization of benzo [a] pyrene diol-epoxide (BPDE)-induced comet assay effects. *Mutagenesis* **2016**, *31* (2), 161–169.

- (54) Yap, C. W. PaDEL-descriptor: an open source software to calculate molecular descriptors and fingerprints. *J. Comput. Chem.* **2011**, 32 (7), 1466–74.
- (55) Saeed, A. I.; Bhagabati, N. K.; Braisted, J. C.; Liang, W.; Sharov, V.; Howe, E. A.; Li, J.; Thiagarajan, M.; White, J. A.; Quackenbush, J. TM4Microarray Software Suite. *Methods Enzymol.* **2006**, *411*, 134–193.
- (56) King, D. J.; Wiseman, A.; Wilkie, D. Studies on the genetic regulation of cytochrome P-450 production in Saccharomyces cerevisiae. *Mol. Gen. Genet.* **1983**, 192 (3), 466–70.
- (57) Kappeli, O. Cytochromes P-450 of yeasts. *Microbiol Rev.* **1986**, 50 (3), 244–258.
- (\$8) Muller-Pillet, V.; Joyeux, M.; Ambroise, D.; Hartemann, P. Genotoxic activity of five haloacetonitriles: comparative investigations in the single cell gel electrophoresis (comet) assay and the amesfluctuation test. *Environ. Mol. Mutagen.* **2000**, *36* (1), 52–8.
- (59) Kundu, B.; Richardson, S. D.; Swartz, P. D.; Matthews, P. P.; Richard, A. M.; Demarini, D. M. Mutagenicity in Salmonella of halonitromethanes: a recently recognized class of disinfection by-products in drinking water. *Mutat. Res., Genet. Toxicol. Environ. Mutagen.* **2004**, *562* (1–2), 39–65.
- (60) Gold, L. S.; Slone, T. H.; Bernstein, L. Summary of Carcinogenic Potency and Positivity for 492 Rodent Carcinogens in the Carcinogenic Potency Database. *Environ. Health Persp* **1989**, 79, 259–272
- (61) Fujita, K.-i.; Kamataki, T. Role of human cytochrome P450 (CYP) in the metabolic activation of N-alkylnitrosamines: application of genetically engineered Salmonella typhimurium YG7108 expressing each form of CYP together with human NADPH-cytochrome P450 reductase. *Mutat. Res., Fundam. Mol. Mech. Mutagen.* **2001**, 483 (1–2), 35–41.
- (62) Pals, J. Mechanisms of monohalogenated acetic acid induced genomic DNA damage; University of Illinois at Urbana-Champaign, 2014.
- (63) Arranz, N.; Haza, A. I.; García, A.; Rafter, J.; Morales, P. Protective effect of vitamin C towards N-nitrosamine-induced DNA damage in the single-cell gel electrophoresis (SCGE)/HepG2 assay. *Toxicol. In Vitro* **2007**, *21* (7), 1311–1317.
- (64) Li, J.; Moe, B.; Vemula, S.; Wang, W.; Li, X.-F. Emerging Disinfection Byproducts, Halobenzoquinones: Effects of Isomeric Structure and Halogen Substitution on Cytotoxicity, Formation of Reactive Oxygen Species, and Genotoxicity. *Environ. Sci. Technol.* **2016**, *50* (13), *6744*–*6752*.
- (65) Kundu, B.; Richardson, S. D.; Granville, C. A.; Shaughnessy, D. T.; Hanley, N. M.; Swartz, P. D.; Richard, A. M.; DeMarini, D. M. Comparative mutagenicity of halomethanes and halonitromethanes in Salmonella TA100: structure—activity analysis and mutation spectra. *Mutat. Res., Fundam. Mol. Mech. Mutagen.* **2004**, 554 (1), 335—350.
- (66) Wang, H.; Wang, X.; Wang, H.; Wang, L.; Liu, A. DFT study of new bipyrazole derivatives and their potential activity as corrosion inhibitors. *J. Mol. Model.* **2006**, *13* (1), 147–153.
- (67) Richard, A. M.; Hunter, E. S. Quantitative structure-activity relationships for the developmental toxicity of haloacetic acids in mammalian whole embryo culture. *Teratology* **1996**, *53* (6), 352–360.